Electronic states in *trans*-polyacetylene with site-type impurities in the coherent-potential approximation

Kikuo Harigaya and Yasushi Wada
Department of Physics, University of Tokyo, 7-3-1 Hongo, Bunkyo-ku, Tokyo 113, Japan

Klaus Fesser
Physikalisches Institut, Universität Bayreuth, Postfach 10 12 51, D-8580 Bayreuth, Federal Republic of Germany
(Received 7 September 1989; revised manuscript received 19 March 1990)

Disorder effects on the electronic states in *trans*-polyacetylene are investigated when site-type impurities are randomly distributed at designated interstitial positions. Use is made of the method previously applied to the bond-type impurities. The generalized Takayama–Lin-Liu–Maki model is studied with the help of the coherent-potential approximation. The dimerization of the lattice is assumed to be represented by a uniform order parameter and the electronic states are half-filled. The order parameter, electronic band structure, density of states, and the total energy are calculated as functions of impurity concentration and strength of the impurity potential. At low concentrations, an impurity band is formed close to either the valence or the conduction band. As the concentration increases, it is connected and absorbed by the latter. When the impurity strength is large enough, the order parameter vanishes in a region around the concentration of 50% together with the energy gap. A phase diagram is given. It has symmetric structure about the 50% concentration.

I. INTRODUCTION

In two earlier papers, we have studied and reported on the properties of polyacetylene with random disorder.[1,2] A generalized Takayama–Lin-Liu–Maki (TLM) model has been investigated with the help of the coherent-potential approximation.[3] When the impurities are of the bond type and give rise to the backward scatterings of electrons, we have found that impurity bands are not formed in the energy gap.[1] This property still remains even when the impurities are of a general type with the site component as well as the bond component.[2] We will later characterize the site component. It induces only forward scatterings. It has been shown that there are no impurity bands as long as the strength of the bond component is larger than that of the site component.[2] When the site component becomes stronger than the bond component, we first find an impurity band in the gap, which is connected either to the valence or the conduction band. It is separated from the latter to become an isolated band, if the site component becomes much stronger.

This property is in striking contrast to the case of semiconductors and superconductors. Since the conducting polymers are quasi-one-dimensional, the Fermi surface is drastically reduced. Electron scatterings by the impurities are limited only to the forward or backward scattering. This is the main reason for the different behaviors.

The purpose of the present paper is to investigate these situations for various impurity concentrations, when the impurities are of the site type. Usually, a site-type impurity is introduced in the Su-Schrieffer-Heeger (SSH) model[4] to give a local potential at the site where the impurity is.[5] Using the connection between the SSH and TLM models,[6] we find that the local potential in the TLM model depends upon whether the impurity is at the $2n$th site or at the $(2n+1)$th site in the SSH model. To avoid the complexity, we assume that the random impurities always occupy interstitial positions between the $2n$th and $(2n+1)$th sites to give the same local potential strength to them. This kind of impurity is named "site type" in Ref. 2 and the present paper.

We use the Soven-Taylor coherent-potential approximation[7] (CPA) on the assumptions that the dimerization pattern of lattice is represented by a uniform order parameter and half of the electronic states are filled. The order parameter is determined self-consistently. The impurity concentration dependences of the order parameter, energy gap, electronic density of states, and the total energy are calculated for various impurity strengths. At low impurity concentrations with a positive impurity strength, we find an isolated impurity band above the valence band. As the concentration increases, it is absorbed by the valence band as the latter intrudes into the gap region. When the impurity strength is large enough, the valence band is connected with the conduction band at a concentration close to 50%, closing the energy gap. This result has symmetry properties around the 50% concentration with respect to the sign of the impurity strength and the valence and conduction bands.

In Sec. II, we present the model and discuss the electronic states around a single impurity. The coherent-potential approximation is applied and numerical results are presented in Sec. III. Section IV is for the discussions.

II. SINGLE-IMPURITY PROBLEM

A site-type impurity gives a local potential at the mth site

$$H_1 = J \sum_s c_{ms}^\dagger c_{ms} \ , \tag{2.1}$$

according to the SSH model.[5] The operator $c_{ms}^\dagger$ creates an electron with spin s at the mth site and J is the strength of the impurity potential. The connection between the two models is[6]

$$\begin{aligned} \Psi_{s1}(R_n) &= (-1)^n (c_{2n,s} + i c_{2n+1,s})/\sqrt{4a} \ , \\ \Psi_{s2}(R_n) &= i(-1)^n (c_{2n,s} - i c_{2n+1,s})/\sqrt{4a} \ , \end{aligned} \tag{2.2}$$

where $R_n = (2n+1/2)a$, a being the undimerized lattice constant in the SSH model. We thus find

$$\begin{aligned} c_{2n,s}^\dagger c_{2n,s} &= a \Psi_s^\dagger(R_n)(1+\sigma_2)\Psi_s(R_n) \ , \\ c_{2n+1,s}^\dagger c_{2n+1,s} &= a \Psi_s^\dagger(R_n)(1-\sigma_2)\Psi_s(R_n) \ , \end{aligned} \tag{2.3}$$

where $\Psi_s(R_n)$ is the field operator of electrons with the two components Ψ_{s1} and Ψ_{s2}, and σ_i are the Pauli matrices. The σ_2 term has a different sign. To avoid the complexity which arises from this difference in a many-impurity system, we assume that the impurities are always at interstitial positions between $2na$ and $(2n+1)a$, giving the same local potential to the two sites. In the single-impurity problem, this assumption replaces (2.1) with

$$H_1 = J \sum_s (c_{2n,s}^\dagger c_{2n,s} + c_{2n+1,s}^\dagger c_{2n+1,s}) \ . \tag{2.4}$$

In the continuum model, it becomes

$$H_1 = U \sum_s \int dx \, \Psi_s^\dagger(x) \delta(x - R_n) \Psi_s(x) \ , \tag{2.5}$$

where $U = 2aJ$. It gives rise only to forward scatterings. We name this kind of impurities "site type."

With many site-type impurities, we get the generalized TLM model Hamiltonian

$$H = H_{\rm TLM} + H_{\rm imp} \ , \tag{2.6}$$

$$H_{\rm TLM} = \sum_s \int dx \, \Psi_s^\dagger(x) \left[-i v_F \sigma_3 \frac{\partial}{\partial x} + \sigma_1 \Delta(x) \right] \Psi_s(x) + \frac{1}{2\pi\lambda v_F} \int dx \, \Delta^2(x) \ , \tag{2.7a}$$

$$H_{\rm imp} = U \sum_i \sum_s \int dx \, \Psi_s^\dagger(x) \delta(x - x_i) \Psi_s(x) \ , \tag{2.7b}$$

where v_F is the Fermi velocity, $\Delta(x)$ is the order parameter, and λ is the dimensionless electron-phonon coupling constant. The coordinate x_i is the location of the ith impurity. The impurities are distributed randomly. We note that the impurity Hamiltonian $H_{\rm imp}$ is different from the corresponding one in the preceding paper[1] as it does not include σ_1.

We first examine a single-impurity problem with a uniform order parameter $\Delta(x) = \Delta_0$. Introducing the Fourier transform by

$$\Psi_s(x) = L^{-1/2} \sum_k e^{ikx} \Psi_s(k) \ ,$$

where L is the system size, we define the temperature Green function in the impurity-free system by

$$G_s^{(0)}(k,\tau) = -\langle T_\tau [\Psi_s(k,\tau) \Psi_s^\dagger(k,0)] \rangle_0 \ , \tag{2.8}$$

where $\Psi_s(k,\tau) = \exp(H_0\tau)\Psi_s(k)\exp(-H_0\tau)$, with $H_0 = H_{\rm TLM} - \mu N_e$, μ and N_e being the chemical potential and total number of electrons, respectively. Its Fourier transform with respect to τ is

$$G_s^{(0)}(k, iE_n) = (iE_n + \mu - v_F k \sigma_3 - \Delta_0 \sigma_1)^{-1} \ , \tag{2.9}$$

where $E_n = (2n+1)\pi T$ is the Matsubara frequency. The Green function for the system with one impurity is

$$G_s(k,p,\tau) = -\langle T_\tau [\tilde{\Psi}_s(k,\tau) \tilde{\Psi}_s^\dagger(p,0)] \rangle \ , \tag{2.10}$$

where $\tilde{\Psi}_s(k,\tau) = \exp(\tilde{H}\tau)\Psi_s(k)\exp(-\tilde{H}\tau)$ with $\tilde{H} = H - \mu N_e$. Its Fourier transform satisfies the equation of motion

$$G_s^{(0)-1}(k, iE_n) G_s(k,p,iE_n) = \delta_{k,p} + \frac{U}{L} \sum_{k'} \exp[i(k'-k)x_0] G_s(k',p,iE_n) \ , \tag{2.11}$$

where x_0 is the coordinate of the impurity. We define a scattering t matrix $t(iE_n)$ by the relation

$$G_s(k,p,iE_n) = \delta_{k,p} G_s^{(0)}(k,iE_n) + G_s^{(0)}(k,iE_n) t(iE_n) G_s^{(0)}(p,iE_n) \ . \tag{2.12}$$

Equation (2.11) gives

$$t(iE_n) = \frac{U}{L} \frac{\exp[i(p-k)x_0]}{1 - \frac{U}{L} \sum_{k'} G_s^{(0)}(k', iE_n)} \ . \tag{2.13}$$

Using (2.9), we obtain

$$\frac{1}{L} \sum_{k'} G_s^{(0)}(k', iE_n) = -\frac{iE_n + \mu + \Delta_0 \sigma_1}{2 v_F [\Delta_0^2 - (iE_n + \mu)^2]^{1/2}} \ . \tag{2.14}$$

Substitution into (2.13) gives

$$t(\omega) = \frac{U}{L} \frac{2 v_F (\Delta_0^2 - \omega^2)^{1/2} [2 v_F (\Delta_0^2 - \omega^2)^{1/2} + \omega U - \Delta_0 U \sigma_1]}{[2 v_F (\Delta_0^2 - \omega^2)^{1/2} + \omega U]^2 - U^2 \Delta_0^2} \exp[i(p-k)x_0] \ , \tag{2.15}$$

where iE_n is replaced by $\omega-\mu$. A localized level around the impurity is determined by the singularity of $t(\omega)$, which is given by

$$(\Delta_0^2-\omega^2)^{1/2}=-\frac{4v_F U\omega}{4v_F^2-U^2} . \tag{2.16}$$

Unless the impurity strength U is unreasonably strong, we may assume

$$4v_F^2>U^2 . \tag{2.17}$$

Equation (2.16) has a solution

$$\omega=-U\left|\frac{\Delta_0}{U}\right|\frac{4v_F^2-U^2}{4v_F^2+U^2} . \tag{2.18}$$

Whether the quantity $U\Delta_0$ is negative or not, there is a localized level. A bond-type impurity does not have a localized level when $U\Delta_0$ is positive, but it has two when $U\Delta_0$ is negative.[1]

III. COHERENT-POTENTIAL APPROXIMATION

We have briefly reviewed the coherent-potential approximation in the preceding paper[1] to obtain the equations which determine the effective-medium Green function $\bar{G}$ and the order parameter Δ. They are applicable to the present problem, after the difference in the type of impurities is taken into account.

The self-energy part of $\bar{G}$ is denoted by Σ, which is called the coherent potential. It is a 2×2 matrix and a function of the Matsubara frequency in the single-site approximation. It satisfies

$$c(J-\Sigma)[1-\bar{g}(J-\Sigma)]^{-1}-(1-c)\Sigma(1+\bar{g}\Sigma)^{-1}=0 , \tag{3.1}$$

where c is the concentration of impurities. The continuum system is simulated by a discrete system with N sites, $2a$ being the lattice constant. The function $\bar{g}$ is defined by

$$\bar{g}(iE_n)=\frac{1}{N}\sum_k \bar{G}(k,iE_n) . \tag{3.2}$$

We can set

$$\Sigma(iE_n)=\Sigma_1(iE_n)1+\Sigma_2(iE_n)\sigma_1 , \tag{3.3a}$$

$$\bar{g}(iE_n)=g_1(iE_n)1+g_2(iE_n)\sigma_1 , \tag{3.3b}$$

and perform the analytic continuations

$$\lim_{iE_n\to\omega-\mu+i\delta}\Sigma(iE_n)=\Sigma(\omega) , \tag{3.4a}$$

$$\lim_{iE_n\to\omega-\mu+i\delta}\bar{g}(iE_n)=\bar{g}(\omega) . \tag{3.4b}$$

It is shown in Ref. 1 that

$$\frac{g_1(\omega)}{\omega-\Sigma_1(\omega)}=\frac{g_2(\omega)}{\Delta+\Sigma_2(\omega)}=-\frac{1}{4\pi t_0 r(\omega)}\left[\mathrm{Ln}\left[\frac{v_F\Lambda-r(\omega)}{-v_F\Lambda-r(\omega)}\right]-\mathrm{Ln}\left[\frac{v_F\Lambda+r(\omega)}{-v_F\Lambda+r(\omega)}\right]\right] , \tag{3.5a}$$

where

$$r(\omega)=[(\omega-\Sigma_1)^2-(\Delta+\Sigma_2)^2]^{1/2} . \tag{3.5b}$$

Here, $v_F=2at_0$ as in the SSH model, the quantity $\Lambda=a^{-1}$ is the cutoff for the k integral and the notation Ln means the principal value. The square root is defined such that $\mathrm{Im}r(\omega)>0$ at the real axis. In the new notations, condition (2.17) is written

$$|J|<2t_0 . \tag{3.6}$$

The self-consistency equation for Δ turns out to be

$$4NT\sum_n g_2(iE_n)+L\frac{\Delta}{\pi\lambda v_F}=0 . \tag{3.7}$$

Introducing the spectral representation

$$g_2(iE_n)=\int_{-\infty}^{\infty}dx\frac{\tau(x)}{iE_n+\mu-x} , \tag{3.8}$$

we rewrite (3.7),

$$\Delta=-4\pi\lambda t_0\int_{-\infty}^{\infty}dx\, f(x-\mu)\tau(x) , \tag{3.9}$$

where $f(x)=1/[\exp(x/T)+1]$ and

$$\tau(x)=-\frac{1}{\pi}\mathrm{Im}g_2(x) . \tag{3.10}$$

At $T=0$ K, Eq. (3.9) becomes

$$\Delta=-4\pi\lambda t_0\int_{-\infty}^{\mu}dx\,\tau(x) . \tag{3.11}$$

Equations (3.1), (3.5a), (3.10), and (3.11) constitute the set of equations to be solved numerically. Equation (3.1) is different from the corresponding equation for the bond-type impurity, J replacing $I\sigma_1$. This is the only difference between the two sets of equations.

In the numerical investigations, we use the parameters $t_0=2.5$ eV, $v_F\Lambda=2t_0$, and $\lambda=0.183$. The order parameter for the impurity-free system is $\Delta_0=2v_F\Lambda\exp(-1/2\lambda)=0.65$ eV. The value of J is varied within $-t_0\lesssim J\lesssim t_0$ and the impurity concentration is in the range $0\le c\le1$. As we show in the Appendix, we can choose a positive value for Δ without loss of generality.

We take 381 points in the mesh of ω space, that is, 50 points for each sign of $\omega-cJ$ in $0.9v_F\Lambda<|\omega-cJ|\le1.2v_F\Lambda$, 40 points for each sign of $\omega-cJ$ in $1.5\Delta<|\omega-cJ|\le0.9v_F\Lambda$, and 201 points for $|\omega-cJ|\le1.5\Delta$. In each energy range, they are evenly

distributed with distance.

First, we take an arbitrary starting value for Δ to get g_1 and g_2 by (3.5a) with the assumptions $\Sigma_1=\Sigma_2=0$. Equation (3.1) is solved to give new Σ_1 and Σ_2, which gives rise to new g_1 and g_2 with the help of (3.5a). The spectral function $\tau(x)$ is calculated by (3.10), which gives a new Δ by (3.11). The process is iterated until the new Δ coincides with the next new Δ within a relative magnitude of 10^{-4}. In the course of the iterations, it is checked that the total number of states does not change more than 0.01%.

In Fig. 1, we present the concentration dependence of the order parameter Δ for six values of $|J|/t_0$. The curves do not depend on the sign of J. They are symmetric with respect to $c=0.5$. These are consequences of symmetries in (3.1) which are shown in the Appendix. The order parameter has a minimum at $c=0.5$. When $|J|/t_0 \gtrsim 0.8$, it vanishes in a region around $c=0.5$.

The electronic density of states per site is calculated by the formula

$$\rho(x)=-\frac{1}{\pi}\mathrm{Tr}\,\mathrm{Im}\bar{g}(x)=-\frac{2}{\pi}\mathrm{Im}g_1(x)\ . \tag{3.12}$$

The number of electrons is given by

$$N_e=2N\int_{-\infty}^{\mu}dx\,\rho(x)\ . \tag{3.13}$$

This determines μ. In Figs. 2(a)–2(c), the positions of the top of the valence band and the bottom of the conduction band are shown by solid and dashed curves, respectively. There are small structures, in Fig. 2(a), on the solid curve at $c\sim 0$ and on the dashed curve at $c\sim 1$. They indicate the impurity bands. The same structures can be found in Figs. 2(b) and 2(c) as well. The band structure shifts upward or downward with the concentration when J is positive or negative, respectively. Figure 2(c) shows that the system becomes gapless in a region around $c=0.5$, if J becomes strong enough. It is associated with the vanishing of Δ, shown in Fig. 1. Typical densities of states are presented in Fig. 3. For a positive J, in the low concentration region, the impurity band is formed close to the valence band. It is absorbed by the valence band already at $c=0.25$. As c increases, the energy of the band edge increases and the density of states becomes rounder. The weight of the density of states shifts upward. Around $c=0.5$, the density of states becomes nonvanishing. For

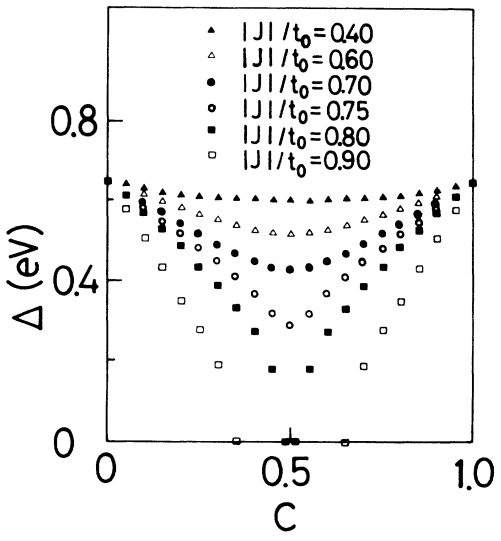

FIG. 1. The order parameter Δ as a function of the impurity concentration and the strength of the impurity potential J.

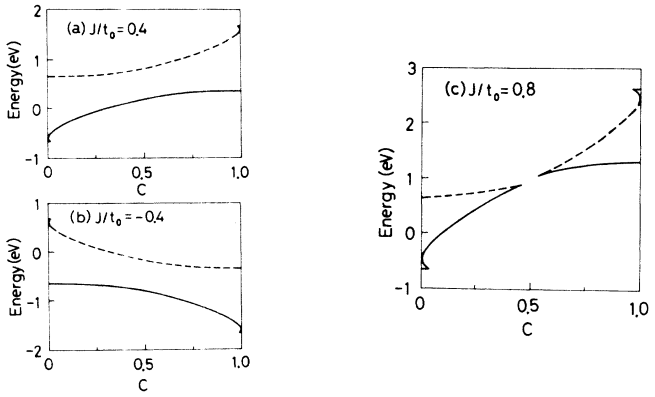

FIG. 2. Positions of the top of the valence band and the bottom of the conduction band as functions of the concentration. The top of the valence band is denoted by the solid line, while the bottom of the concentration band is denoted by the dashed line. Structures at $c\sim 0$ and $c\sim 1$ indicate the formation of isolated impurity bands. The values of the impurity strength are (a) $J/t_0=0.4$, (b) $J/t_0=-0.4$, and (c) $J/t_0=0.8$. The energy gap vanishes in a region around $c=0.5$ in (c).

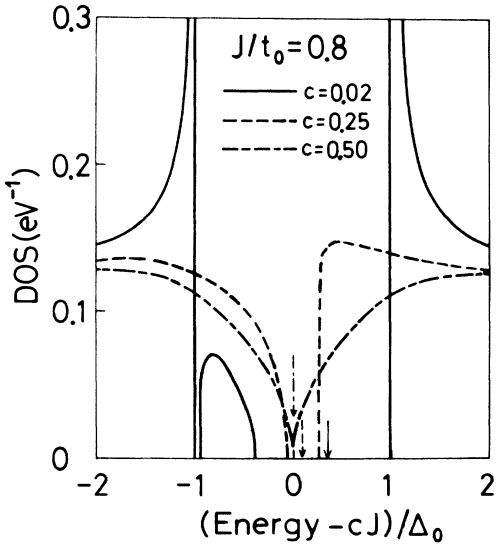

FIG. 3. Density of states per site as a function of the energy and impurity concentration. The impurity strength is $J/t_0=0.8$. The abscissa is energy relative to cJ. For $c>0.5$, the dual symmetry property can be used. The arrow indicates the chemical potential for $c=0.5$. It is in the energy gap specified by the arrow for $c<0.5$.

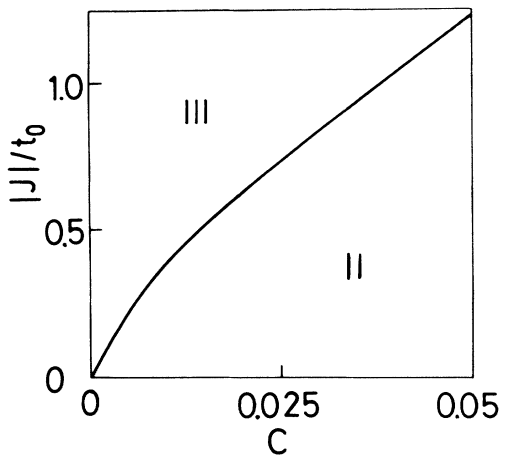

FIG. 4. Phase diagram in the c-J space. In region II, the impurity band is connected either to the valence or to the conduction band. In region III, it is separated.

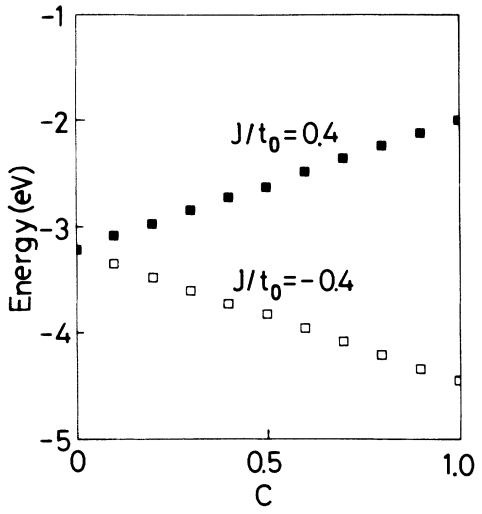

FIG. 6. The energy per site as a function of the impurity concentration for $|J|/t_0=0.4$.

concentrations higher than 0.5, there is a property of the dual symmetry which is discussed in the Appendix. Its structure is symmetric with respect to the point $(c,x)=(0.5,J/2)$. The arrow indicates the chemical potential for $c=0.5$. It is in the energy gap specified by the arrows for $c<0.5$.

For a negative J, in the low concentrations, the impurity band is formed close to the conduction band. As c increases, the weight of the density of states shifts downward. The curves of the band edges are similar to those of the positive J but symmetric with respect to the energy gap.

The concentration at which the isolated impurity band is connected to the valence or conduction band depends on the strength J. In Fig. 4, the relation between c and J is shown. In region II, the impurity band is connected to the valence band for a positive J and a small c. It is isolated in region III. The notations are taken from the preceding paper.[2] Figure 5 is a phase diagram over an extended region. The order parameter Δ vanishes in region IV. It is associated with Fig. 1. The phase boundary for the gapless region is almost the same as the boundary between II and IV.

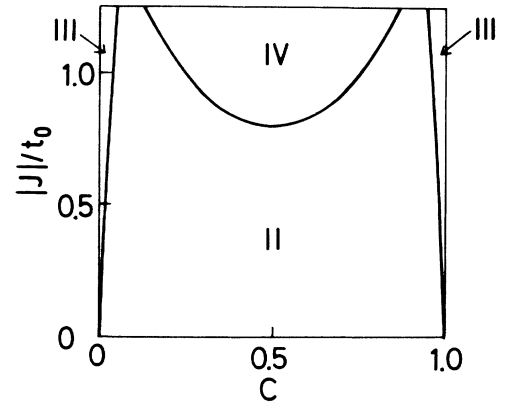

FIG. 5. Phase diagram in the entire space. The order parameter Δ vanishes in region IV. It is practically the same region where the energy gap vanishes; the difference is within the linewidth.

The total energy per site is calculated with the help of the formula

$$E=2\int_{-\infty}^{\mu} dx\, x\rho(x)+\frac{\Delta^2}{2\pi\lambda t_0} . \tag{3.14}$$

The results are shown in Fig. 6. The energy changes linearly with the concentration, because of the shift of the density of states. The electronic energy is changed in the first order of J, while Δ is perturbed only in the second order. The change of the lattice energy is smaller.

IV. DISCUSSIONS

We have found a remarkable difference between the site-type and bond-type impurities. The bond-type impurities have been shown not to make impurity bands, in spite of the fact that a single bond-type impurity has two electronic localized levels in the energy gap, if the order parameter has a different sign from the strength of the impurity potential.[1] In a many-impurity problem, this configuration is not energetically favorable. On the other hand, a single site-type impurity always has a localized level in the gap. When the impurity concentration is small enough, this localized level turns into an isolated impurity band close to the valence or conduction band, if the impurity strength is positive or negative, respectively. We find a similar impurity band when the lattice sites are almost filled by the impurities, the relationship between the band and the sign of impurity strength being reversed. These impurity bands are absorbed by the valence or conduction band as soon as the impurity concentration varies from the extreme values.

The order parameter reduces as the impurity concentration increases. It has a minimum at $c=0.5$. When all the sites are filled by the impurities, we have no disorder.

The total energy simply increases by JN. The disorder is most effective at $c=0.5$. When $|J|$ is larger than $0.8t_0$, the order parameter vanishes in a region around $c=0.5$. The energy gap vanishes at almost the same time. The two phase boundaries are very close to each other. A similar property was reported for superconductors containing magnetic impurities.[8] The critical impurity strength $0.8t_0$ sounds too large. This might be due to the assumption of the uniform dimerization. Numerical simulations have shown that the order parameter deforms asymmetrically at each site-type impurity.[9] It is enhanced at one side of the impurity and reduced at the other side. Thus, in case the order parameter is small enough, it would be possible for gapless regions to develop around the impurities, thereby reducing the critical impurity strength.

When the impurities have the bond and site contributions I and J, respectively, the electronic and band structure becomes more complicated. We showed that the formation of the impurity band in the gap is suppressed if $|I|$ is larger than $|J|$.[2] We named this region I. As $|J|$ becomes larger than $|I|$, we find an impurity band which is connected to the valence or conduction band. This is region II. When $|J|$ becomes much larger, the impurity band is isolated, the region being named III. The boundary between II and III is nearly parallel to $|I|=|J|$ at the concentration $c=0.01$. It crosses the $I=0$ axis at $J\simeq t_0/2$. Figure 4 of the present paper shows the concentration dependence of the crossing point. At a larger concentration, the disorder is more enhanced, leading to a wider impurity band. We then need a larger $|J|$ to have an isolated impurity band.

It would be interesting if the above findings are related to the metal-insulator transition in polyacetylene. Presumably, however, some problems remain to be investigated. One of them is the assumption that the impurities are always at the designated interstitial positions to give the same impurity strength to the $2n$th and $(2n+1)$th sites. This assumption is necessary to get the simple forms, (3.3a) and (3.3b), for the coherent potential and $\bar{g}$, respectively. Otherwise, they would include σ_2 and σ_3 terms. When the impurity concentration is low enough and their potentials are of short range, the impurities would be sparsely distributed. We can neglect the effect of impurity pairs which happen to be at neighboring sites from each other. Each impurity would give a local potential to its closest site. It would be reasonable to assume that half of the impurities give the local potentials to the even-numbered sites and the other half to the odd-numbered sites. The coherent potential and $\bar{g}$ have the simple forms, (3.3a) and (3.3b), in this case, too. We shall show, in a following paper, that the electronic level structure and the phase diagram do not change qualitatively from those in this paper. Another remaining problem would be the necessary generalization of the CPA to include solitons and polarons, as discussed in the previous papers.[1,2] It would also be important to take into account the observed fact that the impurity distribution would not be so random in polyacetylene.[10] How we could take into account the semi random distribution would be a fascinating problem.

ACKNOWLEDGMENTS

One of the authors (Y.W.) would like to thank the University of Bayreuth for their warm hospitality during his visit. Fruitful discussions with Professor Y. Ono, Dr. A. Terai, Dr. K. Iwano, and K. Yonemitsu are acknowledged. This work has been partially supported by a Grant-in-Aid for Scientific Research from the Ministry of Education, Science and Culture, Japan, and by Research Association for Basic Polymer Technology under the sponsorship by NEDO (New Energy and Industrial Technology Development Organization), Japan. It has also been supported by Deutsche Forschungsgemeinschaft (Bonn, Germany) through SFB (Sonderforschungsbereich) 213 (TOPOMAK, Bayreuth). Numerical calculations have been performed on the Fujitsu FACOM-M-380Q computer of the ICEPP (International Center for Elementary Particle Physics), University of Tokyo.

APPENDIX: SYMMETRIES OF THE CPA

Equation (3.1) is rewritten

$$cJ-\Sigma+\bar{g}\Sigma(J-\Sigma)=0\ . \tag{A1}$$

Using (3.3a) and (3.3b), we obtain

$$cJ-\Sigma_1+(g_1\Sigma_1+g_2\Sigma_2)J-g_1(\Sigma_1^2+\Sigma_2^2)-2g_2\Sigma_1\Sigma_2=0 \tag{A2}$$

and

$$-\Sigma_2+(g_1\Sigma_2+g_2\Sigma_1)J-2g_1\Sigma_1\Sigma_2-g_2(\Sigma_1^2+\Sigma_2^2)=0\ . \tag{A3}$$

Equations (A2), (A3), (3.5a), (3.10), and (3.11) are the set of equations solved numerically. We name it the fundamental set, hereafter.

1. Equivalence of two minima of the energy

The fundamental set is invariant with respect to the transformation

$$\Delta\rightarrow-\Delta,\ \Sigma_1\rightarrow\Sigma_1,\ \Sigma_2\rightarrow-\Sigma_2,\ g_1\rightarrow g_1,\ \text{and}\ g_2\rightarrow-g_2\ . \tag{A4}$$

This means

$$\begin{aligned}&\Sigma_1(\omega,-\Delta,J)=\Sigma_1(\omega,\Delta,J)\ ,\\&\Sigma_2(\omega,-\Delta,J)=-\Sigma_2(\omega,\Delta,J)\ ,\\&g_1(\omega,-\Delta,J)=g_1(\omega,\Delta,J)\ ,\\&g_2(\omega,-\Delta,J)=-g_2(\omega,\Delta,J)\ .\end{aligned} \tag{A5}$$

Therefore, these two sets give the same electronic states. The total energy depends only on the absolute magnitude of Δ and the two energy minima with the order parameters $\pm|\Delta|$ are equivalent. We can regard Δ to be positive without loss of generality.

2. Symmetry between the alternative signs of J

The fundamental set is invariant with respect to the transformation

$$\omega\to-\omega,\ \Sigma_1\to-\Sigma_1^*,\ \Sigma_2\to\Sigma_2^*,\ g_1\to-g_1^*,\ g_2\to g_2^*,\ \text{and}\ J\to-J\ . \tag{A6}$$

This means

$$\begin{aligned}\Sigma_1(-\omega,\Delta,-J)&=-\Sigma_1^*(\omega,\Delta,J)\ ,\\ \Sigma_2(-\omega,\Delta,-J)&=\Sigma_2^*(\omega,\Delta,J)\ ,\\ g_1(-\omega,\Delta,-J)&=-g_1^*(\omega,\Delta,J)\ ,\\ g_2(-\omega,\Delta,-J)&=g_2^*(\omega,\Delta,J)\ .\end{aligned} \tag{A7}$$

We have used the fact that

$$r(-\omega)=-r^*(\omega)\ , \tag{A8}$$

since $\mathrm{Im}r(\omega)>0$, and the factor in the parentheses in (3.5a) has the similar property. Therefore, the right-hand side of (3.5a) becomes complex conjugate when ω is replaced by $-\omega$.

In Ref. 1, we introduced the spectral representation for g_2, which gives

$$\mathrm{Im}g_2(\omega)=-\pi\tau_{12}(\omega-\mu)\ , \tag{A9}$$

where

$$\tau_{ij}(x)=\frac{1}{ZN}\sum_{n,n'}\overline{\delta(\varepsilon_n-\varepsilon_{n'}+x)(e^{-\beta\varepsilon_n}+e^{-\beta\varepsilon_{n'}})\sum_k\langle n|\Psi_{si}(k)|n'\rangle\langle n'|\Psi_{sj}^\dagger(k)|n\rangle}\ . \tag{A10}$$

Here, Z is the partition function and ε_m the mth eigenvalue of the one-electron problem (2.6) without the last term of (2.7a), $|m\rangle$ being the corresponding eigenstate, where β is the inverse temperature. We have a sum rule

$$\int_{-\infty}^{\infty}d\omega\,\mathrm{Im}g_2(\omega)=-\frac{\pi}{ZN}\sum_{n,k}\overline{e^{-\beta\varepsilon_n}\langle n|\{\Psi_{s1}(k),\Psi_{s2}^\dagger(k)\}|n\rangle}=0\ . \tag{A11}$$

Equation (3.11) is rewritten

$$\begin{aligned}\Delta&=4\lambda t_0\int_{-\infty}^{\mu}dx\ \mathrm{Im}g_2(x,\Delta,J)\\ &=-4\lambda t_0\int_{\mu}^{\infty}dx\ \mathrm{Im}g_2(x,\Delta,J)\\ &=4\lambda t_0\int_{-\infty}^{-\mu}dx\ \mathrm{Im}g_2(x,\Delta,-J)\ .\end{aligned} \tag{A12}$$

If both μ and $-\mu$ are in the same energy gap where $\mathrm{Im}g_2$ vanishes, Eq. (A12) is identical with (3.11). It means that Δ does not depend on the sign of J.

3. Dual symmetry (Ref. 7)

The fundamental set is invariant with respect to the transformation

$$c\to1-c,\ \omega\to\omega-J,\ \Sigma_1\to\Sigma_1-J,\ \text{and}\ J\to-J\ . \tag{A13}$$

This means

$$\begin{aligned}\Sigma_1(\omega-J,1-c,-J)&=\Sigma_1(\omega,c,J)-J\ ,\\ \Sigma_2(\omega-J,1-c,-J)&=\Sigma_2(\omega,c,J)\ ,\\ g_1(\omega-J,1-c,-J)&=g_1(\omega,c,J)\ ,\\ g_2(\omega-J,1-c,-J)&=g_2(\omega,c,J)\ .\end{aligned} \tag{A14}$$

Using (A7) and (A14), we obtain

$$\begin{aligned}\rho(x,c,J)&=-\frac{2}{\pi}\mathrm{Im}g_1(x,c,J)\\ &=-\frac{2}{\pi}\mathrm{Im}g_1(x-J,1-c,-J)\\ &=-\frac{2}{\pi}\mathrm{Im}g_1(-x+J,1-c,J)\\ &=\rho(-x+J,1-c,J)\ .\end{aligned} \tag{A15}$$

This relation can be used to get the density of states for concentrations higher than 0.5 with the help of Fig. 3.

[1]K. Harigaya, Y. Wada, and K. Fesser, preceding paper, Phys. Rev. B **42**, 1268 (1990).
[2]K. Harigaya, Y. Wada, and K. Fesser, Phys. Rev. Lett. **63**, 2401 (1989).
[3]H. Takayama, Y. R. Lin-Liu, and K. Maki, Phys. Rev. B **21**, 2388 (1980).
[4]W.-P. Su, J. R. Schrieffer, and A. J. Heeger, Phys. Rev. B **22**, 2099 (1980); B **28**, 1138(E) (1983).
[5]S. R. Phillpot, D. Baeriswyl, A. R. Bishop, and P. S. Lomdahl, Phys. Rev. B **35**, 7533 (1987).
[6]S. Kivelson, T.-K. Lee, Y. R. Lin-Liu, I. Peschel, and Lu Yu, Phys. Rev. B **25**, 4173 (1982).
[7]See, for example, F. Yonezawa and K. Morigaki, Suppl. Prog. Theor. Phys. **53**, 1 (1973); J. M. Ziman, *Models of Disorder* (Cambridge University Press, Cambridge, 1979), Chap. 9.
[8]F. Takano, K. Machida, and F. Shibata, Prog. Theor. Phys. **49**,

1077 (1973); F. Takano and K. Fujiki, *ibid.* **49**, 1459 (1973).
[9]Y. Ono, K. Iwano, A. Terai, Y. Ohfuti, and Y. Wada, J. Phys. Soc. Jpn. **58**, 2450 (1989).
[10]L. W. Shacklette and J. E. Toth, Phys. Rev. B **32**, 5892 (1985); M. Winokur, Y. B. Moon, A. J. Heeger, J. Barker, D. C. Bott, and H. Shirakawa, Phys. Rev. Lett. **58**, 2329 (1987); N. S. Murthy, L. W. Shacklette, and R. H. Baughman, Phys. Rev. B **40**, 12 550 (1989).